

Exploring the relationship of brown adipose tissue to bone microarchitecture using 7T MRI and micro-CT

Ping Zhang¹, Baohai Yu¹, Shuying Shao¹, Ranxu Zhang¹, Yan Zeng¹, Jujia Li¹, Congcong Ren¹, Xiaoyue Zhou² and Jian Zhao¹

¹Department of Radiology, The Third Hospital of Hebei Medical University, Hebei Province Biomechanical Key Laboratory of Orthopedics, Shijiazhuang, Hebei and ²Siemens Healthineers Ltd., Shanghai, China

Summary. Background. Brown adipose tissue (BAT) is involved both in energy production and bone metabolism. The purpose of this study was to analyze the relationship between BAT and microarchitecture at cancellous and cortical bone using Kunming mice and the methods of 7T magnetic resonance imaging (MRI) combined with micro-CT.

Methods. Twenty-four female Kunming mice were examined by 7T MRI and measured T2* relaxation time on the deep and superficial interscapular BAT (iBAT) and subcutaneous white adipose tissue (sWAT). Cancellous bone microarchitecture of the distal femur and cortical bone of the middle femur were examined by micro-CT. A paired t-test was used to analyze the differences in T2* values between iBAT and sWAT. The correlation between BAT T2* values and bone microstructure parameters were analyzed using Pearson's correlation.

Results. T2* values of the deep and superficial iBAT (6.36±3.31 ms and 6.23±2.61 ms) were significantly shorter than those of sWAT (16.30±3.05 ms, $t_{\text{deep iBAT}} = -10.816$, $t_{\text{superficial iBAT}} = -12.276$, $p < 0.01$). Deep iBAT T2* values were significantly and negatively correlated with bone volume, cancellous thickness, and bone thickness (Th) and trabecular thickness (Tb.Th) of the cancellous bone of femur. Deep iBAT T2* values were significantly and positively correlated with the structural model index of cancellous bone of femur. Deep iBAT T2* values were significantly and negatively correlated with bone mineral density of the cortical bone of femur.

Conclusions. MRI can distinguish the two adipose tissues from each other. T2* values of BAT were lower than WAT on MRI. BAT related bone remodeling was more correlated with the microstructure of cancellous bone than that of cortical bone.

Key words: Brown adipose tissue, White adipose tissue, Magnetic resonance imaging, Micro-CT, T2* value, Bone microstructure

Introduction

Osteoporosis (OP) is a systemic metabolic bone disease characterized by low bone mass, destruction of bone microstructure, and increased bone fragility (Lane et al., 2000). The initial symptoms are unremarkable. Osteoporosis can lead to bone pain, spinal deformation, fracture, and even disability and death. As the population ages, it is vital that bone mass analytic methods be improved to analyze and prevent OP (Zeytinoglu et al., 2017).

Brown adipose tissue (BAT) is generally found in infants, and levels decrease with age (Marlatt and Ravussin 2017), which can be detected by positron-emitting (18F)-fluorodeoxyglucose (FDG) (Zoch et al., 2016). Functional BAT exists in adults, and its presence is related to heat production. BAT is also present in metabolic diseases, such as obesity and diabetes. BAT has significant negative correlations with BMI and percentage of body fat, and has a significant positive correlation with resting metabolic rate (van Marken Lichtenbelt et al., 2009). Moreover, healthy women with abundant BAT have been shown to have higher mineral bone density than those without abundant BAT, a finding independent of age and compositional body parameters (Lee et al., 2013). To date, the relationship between BAT and bone microstructure has not been studied

Abbreviations. BAT, brown adipose tissue; WAT, white adipose tissue; MRI, magnetic resonance imaging; iBAT, interscapular BAT; sWAT, subcutaneous white adipose tissue; OP, osteoporosis; FDG, fluorodeoxyglucose; BMD, bone mineral density; C/EBP, CCAAT/enhancer-binding protein; BV/TV, bone volume percentage; Tb.Th, trabecular thickness; Tb.Sp, trabecular separation; Tb.N, trabecular number; SMI, structure model index; Ct.Th, cortical bone thickness; Ct.Ar, total cortical bone area; Ct.Po, cortical bone porosity

Corresponding Author: Jian Zhao, Department of Radiology, The Third Hospital of Hebei Medical University, Hebei Province Biomechanical Key Laboratory of Orthopedics, Shijiazhuang, Hebei, China. e-mail: zhaojiansohu@126.com
DOI: 10.14670/HH-18-481



extensively.

Adipose tissue is divided into white adipose tissue (WAT) and BAT based on function. WAT is an energy reservoir that stores lipids in the form of triglycerides, is widely distributed in subcutaneous tissues and around internal organs, and is also an endocrine organ that secretes leptin and angiotensin (Pahlavani et al., 2017). BAT is the main tissue that provides non-shivering thermogenesis in mammals, and is mainly distributed in the neck, supraclavicular, interscapular area, and around the kidneys (Roesler and Kazak, 2020; Yau and Yen, 2020). It is especially abundant in newborns and young mammals (Saely et al., 2012). Brown adipocytes, muscle cells, chondrocytes, and osteoblasts are derived from common mesenchymal stem cells (Pittenger et al., 1999), and BAT is involved in the regulation of stem cell differentiation into the bone lineage cells (Du et al., 2021). UCP-1-deficient mice show significantly decreased cancellous bone mass under mildly cold conditions (Nguyen et al., 2018). In a human study, higher BAT volumes were associated with higher BMD in healthy women (Lee et al., 2013). Young women with BAT had higher BMD and lower Pref-1 compared with women without BAT (Bredella et al., 2012). This finding was not seen in men, and the specific mechanism is not clear. However, the volume of BAT was definitively and positively associated with the amount of bone in children and adolescents. This relationship could be mediated by muscle cells, because BAT was correlated positively with muscle and subcutaneous fat (Ponrartana et al., 2012; Bredella et al., 2014).

BAT is rich in blood supply and mitochondria, so it can be distinguished from WAT using T2* map sequences (Khanna and Branca 2012). Micro-CT can accurately analyze bone microstructure and is widely used *in vitro* to evaluate bone morphology and microstructure (Bouxsein et al., 2010). In this study, we aimed to quantitatively evaluate the distribution and tissue characteristics of iBAT in Kunming mice by 7T MRI. We also sought to study the correlation between the T2* BAT values and cortical and cancellous bone microstructure in middle and distal femurs measured by micro-CT. The results of this study will provide an important evaluation method for the regulation of bone metabolism of brown fat, through MRI imaging displaying brown fat, and quantitative evaluating the brown fat content by functional sequence, combined with micro-CT.

Materials and methods

Animals

To study the general relationship between brown fat and bone structure, ordinary non-immunodeficient Kunming mice were used here. Twenty-four female Kunming mice were provided by the Experimental Animal Center of Hebei Medical University at 5 weeks of age and weighing 20-25 g. They were given SPF

experimental mouse feed with common rat feed (Rat maintenance feed, Feed Code 1022, Beijing Huafukang Biotechnology Co., LTD, China) for 4 months and were maintained in a 12-h light/dark cycle, 22°C room environment. Food and water were provided *ad libitum*. The experimental protocol was approved by the research animal committee of the Third Hospital of Hebei Medical University (S2020-012-1). All methods used were in accordance with the relevant guidelines and regulations.

Fasting for 12 hours was to prevent flatulence and asphyxia caused by excessive secretion in anesthesia, to avoid the special kinetic effects of food on metabolism, then the interscapular area of the mice was examined by 7T MRI; the mice were then sacrificed by intraperitoneal injection of pentobarbital sodium (100 mg/kg) deep anesthesia and immediately dissected. The adipose tissues of BAT and WAT were stained with hematoxylin and eosin, and the distal femur and the mid-diaphysis of femur were examined by micro-CT.

MRI

All mice were scanned on a 7T MR scanner (BioSpec 70/30 USR, Bruker BioSpin MRI GmbH, Ettlingen, Germany) with a mini-imaging gradient coil system. A three-dimensional spoiled-gradient-echo sequence was used with the following parameters: repetition time (TR)=1200 ms, first echo time=4 ms, echo spacing=4-6 ms, echo train length=6, flip angle=50°, FOV=25x30 mm. Interscapular BAT was butterfly-shaped with medium signal intensity, and subcutaneous WAT had a low signal intensity (Fig. 2). T2* values were measured on the transverse section. Then, the largest transverse section of the iBAT and the two adjacent layers were selected. The iBAT was divided into deep and superficial regions, bounded by the middle dividing line, and the average value was calculated. The regions of interest (ROIs) were placed on deep and superficial iBAT and sWAT to avoid any blood vessels and reduce the effect of deoxyhemoglobin on T2* values.

Micro-CT scanning

The soft tissue of the femoral bone was cleaned, and the femur bone was fixed overnight in 70% ethanol. A Skyscan 1176 micro-CT device was used to scan the specimens at 60 kV and 417 μ A. The slice thickness was 8.3 μ m. NRecon version 1.7 and CTAn version 1.17 software were used to reconstruct and analyze images. Cancellous bone of the distal femur was analyzed starting at 150 slices (1.25 mm) proximally from the growth plate and extending 200 slices further (1.66 mm) and in the proximal direction. The cortical bone of mid-diaphysis of femur was analyzed in 200 slices (1.66 mm) and was selected 600 slices (4.99 mm) proximal from the growth plate. The following 3-dimensional parameters were calculated: bone mineral density

Brown adipose tissue and bone microarchitecture

(BMD, mg/cm^3), bone volume percentage (BV/TV, %), trabecular thickness (Tb.Th, mm), trabecular separation (Tb.Sp, mm), trabecular number (Tb.N, $1/\text{mm}$), structure model index (SMI), cortical bone thickness (Ct.Th, mm), cortical area (Ct.Ar, mm^2). The BV/TV is the ratio of the volume of bone tissue to the total ROI volumes. Tb. N, Tb.Th, and Tb.Sp are the three-dimensional morphologic and structural indicators of cancellous bone, among which Tb.Th and Tb.Sp can be used to indicate the thickness and porosity of the cancellous bone. SMI is used to evaluate the plates and rod shapes of the cancellous bone structure.

Histologic analysis

Interscapular and subcutaneous fat tissues were resected and fixed in 10% buffered formalin for 24 h. The tissues were then dehydrated with gradient alcohol, embedded in paraffin, and cut into 4- μm thick sections. The sections were stained for hematoxylin and eosin. Adipocyte morphology was observed with a microscope.

Statistical analyses

Statistical analyses were conducted using SPSS v.17.0 (Chicago, IL) software. Results were expressed as the mean \pm standard deviation. A Kolmogorov-Smirnov test was used to confirm that the data were normally distributed ($p > 0.05$). The paired-sample t-test was used to compare the $T2^*$ relaxation parameters of deep and superficial iBAT vs sWAT, and was two-tailed. Using G*Power and identifying an alpha level of 0.05, an effect size of 3.12, and a sample size of 24, the post hoc statistical power was 1.00. Pearson's correlation was used to analyze the correlations between $T2^*$ relaxation

time of iBAT and the BMD, BV/TV, Tb. Th, Tb.Sp, Tb. N, Ct.Th, and Ct.Ar. A $p < 0.05$ indicated a statistically significant difference.

Results

Histologic observations

The subcutaneous fat was composed primarily of white adipocytes. The fat in the interscapular region consisted primarily of brown adipocytes, with few white adipocytes. Brown fat loses its typical bubbly lipid droplets, which fuse into individual cells morphologically similar to white fat cells but with smaller cell diameters (Fig. 1).

$T2^*$ and micro-CT

There was no significant difference between the $T2^*$ value of deep BAT and shallow BAT (6.36 ± 3.31 ms vs 6.23 ± 2.61 ms, $n = 24$, $t = 0.427$, $p = 0.674$). $T2^*$ values of the deep and superficial iBAT were significantly shorter than those of sWAT (16.30 ± 3.05 ms, $t_{\text{deep iBAT}} = -10.816$, $t_{\text{superficial iBAT}} = -12.276$, $p < 0.01$). The deep and superficial iBAT had a significantly shorter $T2^*$ value than subcutaneous WAT.

The bone microstructure data of the cancellous bone of distal femur were as follows: BMD = 0.23 ± 0.06 mg/cm^3 ; BV/TV = $39.22 \pm 10.92\%$; Tb.Th = 0.18 ± 0.02 mm; Tb.N = 2.21 ± 0.51 $1/\text{mm}$; Tb.Sp = 0.51 ± 0.27 mm; SMI = 1.22 ± 0.51 . The Pearson correlation analysis between iBAT $T2^*$ value and the cancellous bone of the distal femur indicated significant negative correlations between deep iBAT $T2^*$ values and BV/TV, Tb.Th, Tb.N, and significant positive correlations between deep

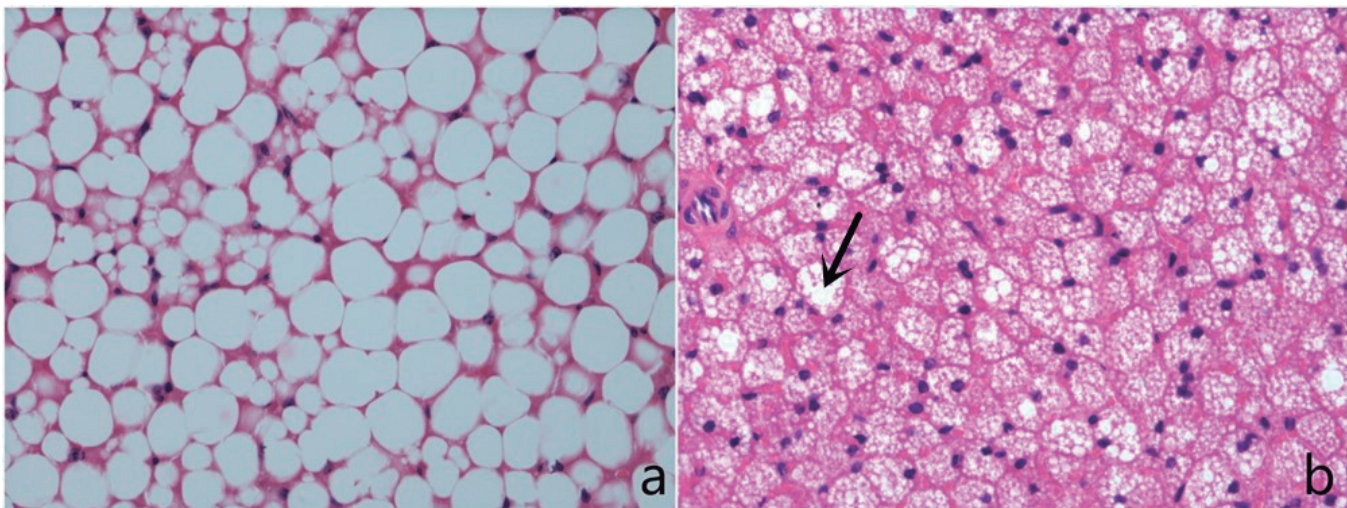


Fig. 1. H&E-stained sections: The subcutaneous WAT from the scapular region contained white adipocytes (a) and deep iBAT from the scapular region contained mostly brown adipocytes (b), but also some white adipocytes (indicated by the arrow). $\times 400$.

iBAT T2* value and SMI. There were no significant correlations between deep iBAT T2* and Tb.Sp. There was a significant negative correlation between superficial iBAT T2* value and Tb.N. There were no significant correlations between superficial iBAT T2* value and BMD, BV/TV, Tb.Th, Tb.Sp, and SMI (Table 1).

The bone microstructure data of the cortical bone of mid-diaphysis of femur were as follows: BMD=0.37±0.06 mg/cm³; Ct.Th=0.27±0.04 mm; Ct.Ar=9.73±0.85 mm². Based on the Pearson correlation analysis between iBAT T2* value and cortical bone of mid-diaphysis of femur, there was a significant correlation between deep iBAT T2* value and BMD. There were no significant correlations between deep iBAT T2* and Ct.Th, Ct.Ar. There were no significant correlations between superficial iBAT T2* and BMD, Ct.Th, or Ct.Ar (Table 2).

sWAT had no significant correlations with BMD, BV/TV, Tb.Th, Tb.Sp, or SMI of cancellous bone of the distal femur. sWAT had no significant correlations with BMD, Ct.Th, or Ct.Ar of cortical bone of mid-diaphysis of femur (Tables 1, 2).

Discussion

PET/CT is the most commonly used method to detect the location and activation status of BAT; however, it requires intravenous injections and ionizing radiation exposure, which especially limits its use in children. The volume of BAT is positively associated with the amount of bone and the cross-sectional size of

femoral bone structure (Ponrartana et al., 2012; Bredella et al., 2014). 7T MRI is non-invasive and provides better spatial resolution, faster acquisition speeds, and more stable image quality than PET/CT (Gu et al., 2020). In this study, T2* map sequence of 7T MRI clearly distinguished BAT from WAT. BAT was located on the dorsal side of the interscapular region, with a butterfly shape, slightly low signal intensity, and small blood vessels. sWAT had a lower signal intensity (Fig. 2). The deep and superficial iBAT had significantly shorter T2*

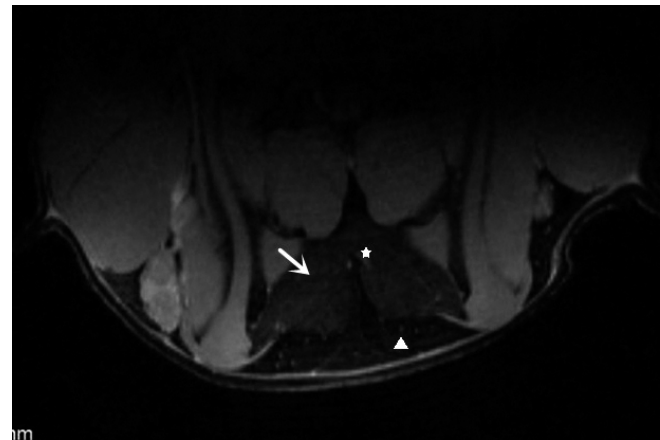


Fig. 2. The interscapular BAT was shown as butterfly-shaped and medium intensity signal (straight arrow). The blood vessels had a slightly higher signal intensity (asterisk), and the subcutaneous WAT had a low signal intensity (triangle).

Table 1. Pearson correlations between iBAT and sWAT T2* value with bone microstructure of the distal femur.

| Parameters | deep iBAT T2*(n=24) | superficial iBAT T2* (n=24) | sWAT T2*(n=24) |
|---------------------------|---------------------|-----------------------------|----------------|
| BMD (mg/cm ³) | -0.241(0.257) | -0.151(0.481) | -241(0.257) |
| BV/TV (%) | -0.554(0.005*) | -0.387(0.062) | -0.163(0.446) |
| Tb.Th (mm) | -0.413(0.045*) | -0.216(0.311) | 0.014(0.950) |
| Tb.N (1/mm) | -0.542(0.006*) | -0.406(0.049*) | -0.161(0.452) |
| Tb.Sp (mm) | 0.124(0.056) | 0.056(0.795) | 0.375(0.071) |
| SMI | 0.465(0.022*) | 0.331(0.114) | 0.279(0.187) |

*, The correlations that were significant, P<0.05. Data are presented as Pearson correlation coefficient (p-value). iBAT, interscapular brown adipose tissue, sWAT, subcutaneous white adipose tissue, BMD, bone mineral density, BV/TV, bone volume percentage, Tb.Th, trabecular thickness, Tb.N, trabecular number, Tb.Sp, trabecular separation, SM, structure model index.

Table 2. Pearson correlation between iBAT and sWAT T2* relaxation times with bone microstructure of mid-diaphysis of femur

| Parameters | deep iBAT T2*(n=24) | superficial iBAT T2*(n=24) | sWAT T2*(n=24) |
|---------------------------|---------------------|----------------------------|----------------|
| BMD (mg/cm ³) | -0.483(0.017*) | -0.349(0.095) | -0.159(0.457) |
| Ct.Th (mm) | -0.105(0.625) | -0.016(0.942) | -0.129(0.549) |
| Ct.Ar (mm ²) | -0.047(0.829) | 0.192(0.369) | -0.281(0.183) |

*, The correlations that were significant, P<0.05. Data are presented as Pearson correlation coefficient (p-value). iBAT, interscapular brown adipose tissue, sWAT, subcutaneous white adipose tissue, BMD, bone mineral density, Ct.Th, cortical bone thickness, Ct.Ar, cortical area.

values compared with the subcutaneous WAT, which was consistent with other research studies. For example, iBAT T2* values were lower than those of gonadal WAT in thin and obese mice using 3T MRI (Hu et al., 2012). In a human study using 3T PET / MRI, T2 values of supraclavicular BAT was significantly lower than that of sWAT (Holstila et al., 2017). BAT T2* values were also lower than WAT in another study, which could have been due to the different amounts of intracellular iron, blood oxygenation, and perfusion in the tissues between BAT and WAT (Hu et al., 2013), making the signal intensity different between the two adipose tissues on MRI.

In this study, there was no consensus about the findings pertaining to deep and superficial iBAT. BAT is the main tissue that provides non-shivering thermogenesis. The different fat cell types in the body can be transformed into each other under cold exposure, exercise, tumor load and other conditions, and the color and size of the fat deposits in mice can change significantly under cold conditions. Although cold exposure did not change the total number of fat cells in the fat organs, it did significantly increase the number of brown fat cells, while the number of white fat cells decreased correspondingly, which indicated a differentiation and transfer process from white adipocytes to brown adipocytes in cold-exposed mice (Murano et al., 2009). MRI can be used to non-invasively assess BAT structure and function (Wu et al., 2020). T2* signal intensities can be used to determine the distribution of brown fat (Hui et al., 2017). T2* values and proton density fat-fractions are lower in BAT than WAT (Hu et al., 2012), and T2* relaxation times of activated BAT decrease significantly compared with not activated BAT (Hu et al., 2021). In this study, there were no significant differences between deep and superficial iBAT T2* values. In addition, the superficial iBAT T2* value tended to be lower than that for deep iBAT. The low T2* value of BAT was related to the deposits and activity (Hu et al., 2013, 2021). That is to say, the deposits and activity of superficial iBAT were higher than deep iBAT.

BAT might play an indirect role in age-related bone loss. However, evidence of an indirect effect from thermogenic dysfunction on bone loss is currently limited (Motyl and Rosen, 2011). What is more bone morphogenic proteins (BMPs) play an important role in adipogenesis. BMP7 triggers commitment of progenitor cells to a brown adipocyte lineage and activates brown adipogenesis. BMP4 plays an important role in promoting brown adipocyte differentiation and thermogenesis in vivo and in vitro (Xue et al., 2014). Here, we present current evidence for a relationship between BAT and bone micro structure. In this study, the deep iBAT T2* value was more significantly correlated with the cancellous bone than cortical bone. That is to say, BAT-related bone remodeling begins with cancellous bone. SMI value of parallel plates is close to 0, and that of cylindrical rods is close to 3 (Bouxsein et al., 2010). In this study, there was a significant positive

correlation between deep iBAT T2* values and SMIs of the distal femur, indicating that BAT was positively correlated with cancellous structural stability. This might explain why the correlation between BAT and cancellous bone was better than that of the cortical bone data in this study. What's more, changes in bone mass related to loading and unloading were more pronounced in cancellous than cortical bone (Yang et al., 2019). Thus, cancellous bone appears to be more sensitive to transient stress than cortical bone.

This study had the following limitations. First, the age was not considered. The dynamic changes in T2* values and bone mass related to age should be examined in future studies. The brown fat was only moderately associated with bone microstructure. The effect of WAT distributions on bone mass was not considered.

Conclusions

MRI can distinguish brown fat from white fat by T2* value. T2* value of brown fat was significantly lower than that of white fat. Brown fat is associated with cancellous bone structure, suggesting that brown fat-related remodeling may begin in cancellous bone.

Acknowledgements and Funding. Not Applicable

Competing interest. There is no conflict of interest.

Authors' contributions. JZ and PZ designed the experimental scheme. BY and JC revised this article. SS and RZ analyzed the imaging data, and were the major contributors in writing the manuscript. YZ, JL and CR performed the histological examination of the fat.

Ethics approval and consent to participate. This study was approved by the Ethics Committee of the Third Hospital of Hebei Medical University. The committee's number was 2019-003-1.

References

- Bouxsein M.L., Boyd S.K., Christiansen B.A., Guldberg R.E., Jepsen K.J. and Müller R. (2010). Guidelines for assessment of bone microstructure in rodents using micro-computed tomography. *J. Bone Miner. Res.* 25, 1468-1486.
- Bredella M.A., Fazeli P.K., Freedman L.M., Calder G., Lee H., Rosen C.J. and Klibanski A. (2012). Young women with cold-activated brown adipose tissue have higher bone mineral density and lower Pref-1 than women without brown adipose tissue: a study in women with anorexia nervosa, women recovered from anorexia nervosa, and normal-weight women. *J. Clin. Endocrinol. Metab.* 97, E584-590.
- Bredella M.A., Gill C.M., Rosen C.J., Klibanski A. and Torriani M. (2014). Positive effects of brown adipose tissue on femoral bone structure. *Bone* 58, 55-58.
- Du J., He Z., Xu M., Qu X., Cui J., Zhang S., Zhang S., Li H. and Yu Z. (2021). Brown adipose tissue rescues bone loss induced by cold exposure. *Front Endocrinol. (Lausanne)* 12, 778019.
- Gu J., Wang X., Yang H., Li H. and Wang J. (2020). Preclinical in vivo imaging for brown adipose tissue. *Life Sci.* 249, 117500.
- Holstila M., Pesola M., Saari T., Koskensalo K., Raiko J., Borra R.J., Nuutila P., Parkkola R. and Virtanen K.A. (2017). MR signal-fat-

- fraction analysis and T2* weighted imaging measure BAT reliably on humans without cold exposure. *Metabolism* 70, 23-30.
- Hu H.H., Hines C.D., Smith D.L., Jr. and Reeder S.B. (2012). Variations in T(2)* and fat content of murine brown and white adipose tissues by chemical-shift MRI. *Magn. Reson. Imaging* 30, 323-329.
- Hu H.H., Yin L., Aggabao P.C., Perkins T.G., Chia J.M. and Gilsanz V. (2013). Comparison of brown and white adipose tissues in infants and children with chemical-shift-encoded water-fat MRI. *J. Magn. Reson. Imaging* 38, 885-896.
- Hu Q., Cao H., Zhou L., Liu J., Di W., Lv S., Ding G. and Tang L. (2021). Measurement of BAT activity by targeted molecular magnetic resonance imaging. *Magn. Reson. Imaging* 77, 1-6.
- Hui S.C.N., Ko J.K.L., Zhang T., Shi L., Yeung D.K.W., Wang D., Chan Q. and Chu W.C.W. (2017). Quantification of brown and white adipose tissue based on Gaussian mixture model using water-fat and T2* MRI in adolescents. *J. Magn. Reson. Imaging* 46, 758-768.
- Khanna A. and Branca R.T. (2012). Detecting brown adipose tissue activity with BOLD MRI in mice. *Magn. Reson. Med.* 68, 1285-1290.
- Lane J.M., Russell L. and Khan S.N. (2000). Osteoporosis. *Clin. Orthop. Relat. Res.* 139-150.
- Lee P., Brychta R.J., Collins M.T., Linderman J., Smith S., Herscovitch P., Millo C., Chen K.Y. and Celi F.S. (2013). Cold-activated brown adipose tissue is an independent predictor of higher bone mineral density in women. *Osteoporos. Int.* 24, 1513-1518.
- Marlatt K.L. and Ravussin E. (2017). Brown adipose tissue: an update on recent findings. *Curr. Obes. Rep.* 6, 389-396.
- Motyl K.J. and Rosen C.J. (2011). Temperatures rising: brown fat and bone. *Discov. Med.* 11, 179-185.
- Murano I., Barbatelli G., Giordano A. and Cinti S. (2009). Noradrenergic parenchymal nerve fiber branching after cold acclimatisation correlates with brown adipocyte density in mouse adipose organ. *J. Anat.* 214, 171-178.
- Nguyen A.D., Lee N.J., Wee N.K.Y., Zhang L., Enriquez R.F., Khor E.C., Nie T., Wu D., Sainsbury A., Baldock P.A. and Herzog H. (2018). Uncoupling protein-1 is protective of bone mass under mild cold stress conditions. *Bone* 106, 167-178.
- Pahlavani M., Kalupahana N.S., Ramalingam L. and Moustaid-Moussa N. (2017). Regulation and functions of the renin-angiotensin system in white and brown adipose tissue. *Compr. Physiol.* 7, 1137-1150.
- Pittenger M.F., Mackay A.M., Beck S.C., Jaiswal R.K., Douglas R., Mosca J.D., Moorman M.A., Simonetti D.W., Craig S. and Marshak D.R. (1999). Multilineage potential of adult human mesenchymal stem cells. *Science* 284, 143-147.
- Ponrartana S., Aggabao P.C., Hu H.H., Aldrovandi G.M., Wren T.A. and Gilsanz V. (2012). Brown adipose tissue and its relationship to bone structure in pediatric patients. *J. Clin. Endocrinol. Metab.* 97, 2693-2698.
- Roesler A. and Kazak L. (2020). UCP1-independent thermogenesis. *Biochem. J.* 477, 709-725.
- Saely C.H., Geiger K. and Drexel H. (2012). Brown versus white adipose tissue: a mini-review. *Gerontology* 58, 15-23.
- van Marken Lichtenbelt W.D., Vanhomerig J.W., Smulders N.M., Drossaerts J.M., Kemerink G.J., Bouvy N.D., Schrauwen P. and Teule G.J. (2009). Cold-activated brown adipose tissue in healthy men. *N. Engl. J. Med.* 360, 1500-1508.
- Wu M., Junker D., Branca R.T. and Karampinos D.C. (2020). Magnetic resonance imaging techniques for brown adipose tissue detection. *Front. Endocrinol. (Lausanne)* 11, 421.
- Xue R., Wan Y., Zhang S., Zhang Q., Ye H. and Li Y. (2014). Role of bone morphogenetic protein 4 in the differentiation of brown fat-like adipocytes. *Am. J. Physiol. Endocrinol. Metab.* 306, E363-372.
- Yang H., Xu X., Bullock W. and Main R.P. (2019). Adaptive changes in micromechanical environments of cancellous and cortical bone in response to in vivo loading and disuse. *J. Biomech.* 89, 85-94.
- Yau W.W. and Yen P.M. (2020). Thermogenesis in adipose tissue activated by thyroid hormone. *Int. J. Mol. Sci.* 21, 3020.
- Zeytinoglu M., Jain R.K. and Vokes T.J. (2017). Vertebral fracture assessment: Enhancing the diagnosis, prevention, and treatment of osteoporosis. *Bone* 104, 54-65.
- Zoch M.L., Abou D.S., Clemens T.L., Thorek D.L. and Riddle R.C. (2016). In vivo radiometric analysis of glucose uptake and distribution in mouse bone. *Bone Res.* 4, 16004.